FRIEDRICH-ALEXANDER
UNIVERSITÄT
ERLANGEN-NÜRNBERG

FACULTY OF ENGINEERING

Intelligent Reflecting Surfaces for Free-space Optical Communications

One World Signal Processing Seminar Series 2021

Marzieh Najafi, Hedieh Ajam, Vahid Jamali, Bernhard Schmauss, and Robert Schober
Friedrich-Alexander-University (FAU) of Erlangen-Nürnberg, Germany
September 29, 2021

Outline

1. Introduction to FSO Systems

FSO Systems

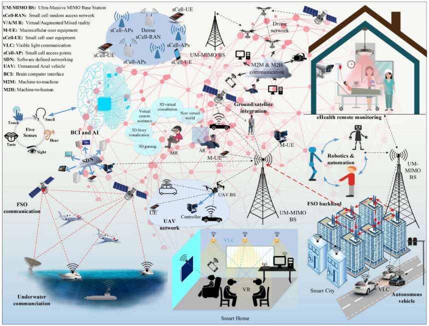

Figure: Possible 6G architecture[1].

- **Applications**
  - Last-mile access
  - Fiber backup
  - Backhaul of wireless networks
  - Satellite communications
  - Drone communication
- **Advantages**
  - Directional narrow laser beams
  - Cost-efficient transceivers
  - Link coverage ($>$ 1000 km)
  - License-free bandwidth
  - High data rates (up to 10 Gbps)

[1] M. Z. Chowdhury, M. Shahjalal, S. Ahmed, and Y. M. Jang, "6G wireless communication systems: Applications, requirements, technologies, challenges, and research Directions," in *IEEE Open J. Commun. Soc.*, vol. 1, 2020.

Limitations in FSO Systems

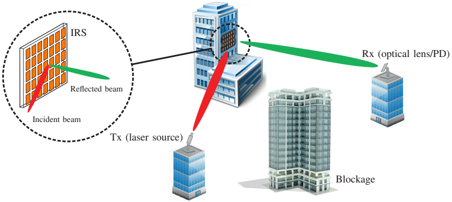

- **Limiting factors**
  - Atmospheric turbulence
  - Adverse whether conditions
  - Beam divergence
  - Misalignment errors
  - Line-of-sight (LOS) connection
- **Countermeasures**
  - MIMO FSO systems
  - Hybrid RF/FSO systems
  - Serial and parallel FSO relays
  - Optical IRSs

2. Optical IRSs

Optical Reflecting Surfaces

Possible realizations:

- Mirror-based IRSs:
  - Standard mirrors
  - Micro-mirrors
- Meta-surface-based IRSs:
  - Non-reconfigurable meta-surfaces
  - Reconfigurable meta-surfaces

Standard Mirrors

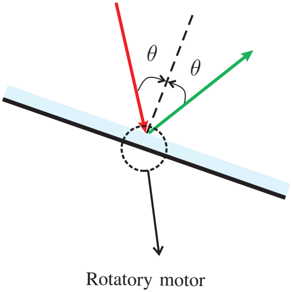

- Physical operating principle:
  - Specular reflection
  - Mechanical re-orientation
- Control resolution $>$ 1 cm
- Low functional capability
- Low tunability
- Cheap and technologically mature

Micro-Mirrors

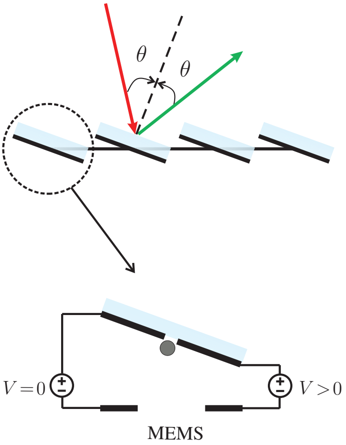

- Physical operating principle:
  - Specular reflection
  - Mechanical re-orientation via MEMS
- Control resolution $>$ 1 mm
- Moderate functional capability
- Moderate tunability
- Technologically mature (not for the FSO applications in this talk)

Non-reconfigurable Meta-Surfaces

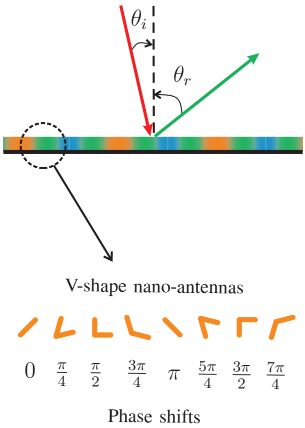

- Physical operating principle:
  - Nano-antennas (on the order of sub-wavelength)
  - Change of geometrical properties (size, orientation, etc.)
- Control resolution $>$ 500 nm
- High functional capability
- **No** tunability
- Various proofs-of-concept available but technologically not mature

Reconfigurable Meta-Surfaces

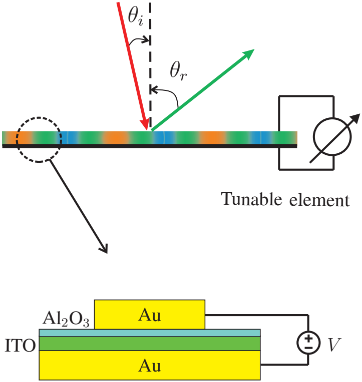

- Physical operating principle (change of material properties):
  - Charge density (e.g., conductive oxide materials or graphene)
  - Structure (phase-transition materials)
  - Molecular alignment (liquid crystal)
- Control resolution $> 1 - 10$ µm
- High functional capability
- High tunability
- Various proofs-of-concept available but technologically not mature

FRIEDRICH-ALEXANDER UNIVERSITÄT ERLANGEN-NÜRNBERG
FACULTY OF ENGINEERING

Optical vs. RF IRSs

Various differences including:

- IRS electrical size
- Analysis methods
- Type of incident waves
- Channel impairments

IRS Electrical Size

- **IRS electrical size L_e:**

$$L_e = \frac{L}{\lambda}$$

  - L: IRS size in meter
  - λ: Wavelength in meter

- **Example:**
  - 10 cm at 3 GHz (sub-6 GHz), 30 GHz (mmWave), 3 THz (THz), and 300 THz (optical) correspond to 1, 10, 1000, 100000 wavelengths, respectively

- **Important consequences (from a theoretical point-of-view):**
  - High flexibility in terms of beam shaping
  - Analysis techniques based on geometric-optics may become accurate

Analysis Methods: Scattering Theory vs. Geometric Optics

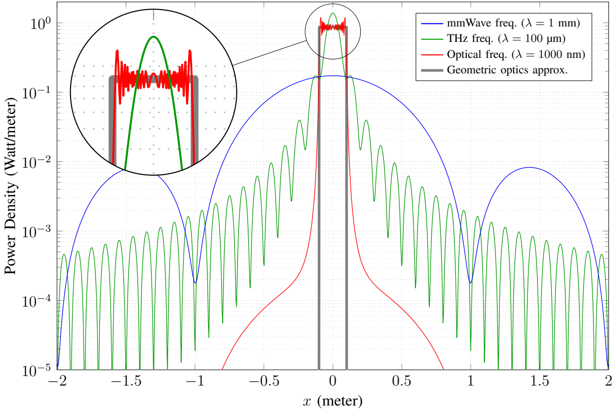

Power density of the reflected wave at x and $y = 200$ m. An IRS located at origin on the x-axis with size 20 cm anomalously reflects an oblique plane wave impinged from angle 30° into perpendicular direction [R1].

Incident Wave Models

- **Wave models**
  - RF: Plane or spherical waves
  - FSO: Concentrated wave models such as the Gaussian beam
- **Consequence**
  - E.g.: Saturated performance gain in terms of IRS size

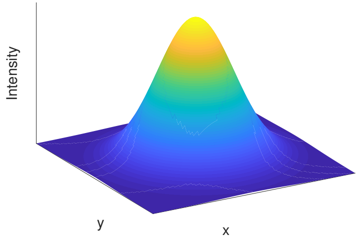

Channel Impairments

- **RF systems**
  - Free-space path-loss
  - Multi-path fading
  - Random shadowing
  - Atmospheric loss (e.g., in mmWave)
  - ✗
  - ✗

- **FSO systems**
  - Geometric loss (divergence of the beam)
  - ✗
  - ✗
  - Atmospheric loss (dominant factor in low-visibility conditions (e.g., fog))
  - Atmospheric turbulence-induced fading
  - Pointing errors and misalignment losses

Design Goals

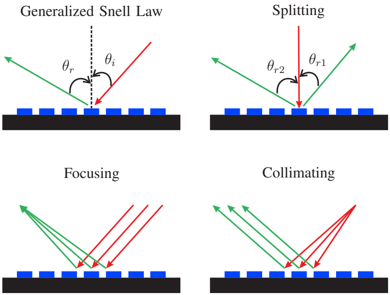

Goals:

- Relaxing LoS requirement
- Supporting multiple links
- Re-adjusting beamwidth
- Correcting distorted wavefront
- Maximizing Rx's received power
- ...

Considerations:

- Gaussian beam
- Building sway
- ...

3. Modeling of IRS-assisted FSO Links

IRS-assisted FSO Link

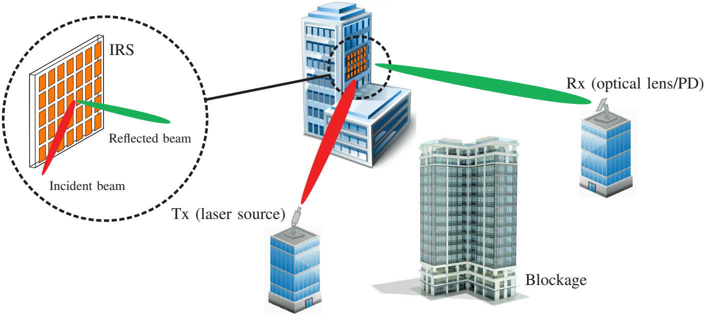

Question: How much of the transmitted optical power in an IRS-assisted FSO link can be collected at the receiver lens?

Transmitter

Gaussian beam (emitted from the origin and propagating along the z-axis):

$$E(a,z) = E_0 \left(\frac{w_0}{w(z,w_0)} \right)^{\frac{n-1}{2}} \exp\left(-\frac{a^2}{w^2(z,w_0)} \right) \times \exp\left(-j \left(kz + k \frac{a^2}{2R(z,w_0)} - \psi(z,w_0) \right) \right), \quad n \in \{2,3\}$$

- $n \in \{2,3\}$: Dimension of the space (i.e., 2D or 3D)
- a: Distance to the center of beam footprint (2D: $a = x$, 3D: $a = \sqrt{x^2 + y^2}$)
- E_0: Electric field at the origin
- w_0: Beam waist radius
- $w(z,w_0)$: Beamwidth at distance z
- k: Wave number
- $R(z,w_0)$: Curvature radius of the beam's wavefront at distance z
- $\psi(z,w_0)$: Near-field Gouy phase (becomes constant for large z)

Transmitter

Gaussian beam (emitted from the origin and propagating along the z-axis):

$$E(a,z) = E_0 \left(\frac{w_0}{w(z,w_0)} \right)^{\frac{n-1}{2}} \exp\left(-\frac{a^2}{w^2(z,w_0)} \right) \times \exp\left(-j \left(kz + k\frac{a^2}{2R(z,w_0)} - \psi(z,w_0) \right) \right), \quad n \in \{2,3\}$$

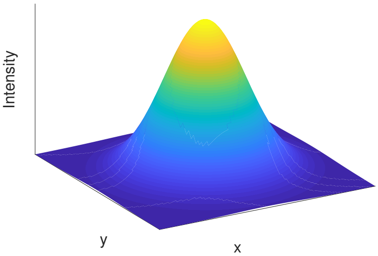

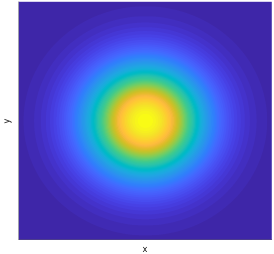

Receiver

Direct detection:

$$h_g = \iint_{(x,y)\in\mathscr{A}} I(x,y)\mathrm{d}x\mathrm{d}y$$

- $\mathscr{A}$: Receiving lens area
- $I(x,y)$: Power intensity on the Rx lens plane

$$I(x,y) = \frac{|E^{\text{lens}}(x,y)|^2}{2\eta}$$

- $E^{\text{lens}}(x,y)$: Electric field on the lens
- η: Free-space impedance

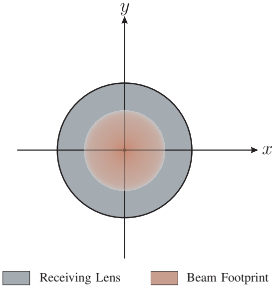

Analysis Methods

- **Scattering theory**
  - IRS as a collection of discrete phase-shifting unit-cells
- **Huygens-Fresnel principle**
  - IRS as a continuous phase-shifting surface
- **Geometric optics**
  - Approximating the reflection of waves from the IRS based on ray optics

Scattering theory

Reflected electrical field:

$$E^{\mathrm{lens}}(\mathbf{r}) = \sum_m \sqrt{s^{\mathrm{irs}}(E_m^{\mathrm{irs}})} \frac{\exp(jk|\mathbf{r}-\mathbf{p}_m|)}{|\mathbf{r}-\mathbf{p}_m|^{\frac{n-1}{2}}} \exp(j\phi_m),$$

- $E^{\mathrm{lens}}(\mathbf{r})$: Electric field at the Rx lens at position $\mathbf{r}$
- E_m^{irs}: Incident field on the m-th unit cell
- $s^{\mathrm{irs}}(\cdot)$: Power of the reflected wave
- $\mathbf{p}_m$: Position of the m-th unit cell
- ϕ_m: Phase of the reflected wave from the m-th unit cell
- $n \in \{2,3\}$: Dimension of the space (i.e., 2D or 3D)
- k: Wave number

Huygens-Fresnel principle

Reflected electrical field:

$$E^{\text{lens}}(\mathbf{r}) = \frac{\varsigma}{j\lambda^{\frac{n-1}{2}}} \int_{\mathbf{p}\in\mathscr{A}^{\text{irs}}} E^{\text{irs}}(\mathbf{p}) \frac{\exp(jk|\mathbf{r}-\mathbf{p}|)}{|\mathbf{r}-\mathbf{p}|^{\frac{n-1}{2}}} \exp(j\Delta\phi(\mathbf{p}))\mathrm{d}\mathbf{p},$$

- $E^{\text{lens}}(\mathbf{r})$: Electric field at the Rx lens at position $\mathbf{r}$
- $E^{\text{irs}}(\mathbf{p})$: Incident field at position $\mathbf{p}$ on the IRS
- ς: A factor to ensure IRS passivity
- $\mathscr{A}^{\text{irs}}$: Set of points on the IRS
- $\Delta\phi_m$: Phase-shift of the m-th unit cell
- $n \in \{2,3\}$: Dimension of the space (i.e., 2D or 3D)
- k: Wave number

Geometric Optics

Basic idea: Approximating wave propagation by ray tracing

What is a ray?

- **Ideal:** Wave propagation in a certain direction with zero beamwidth
- **Pragmatic:** Wave propagation in a certain direction with a beamwidth smaller than the largest dimension of interest

The beamwidth is inversely proportional to the electric dimension of the EM radiator (e.g., IRS)
$\Longrightarrow$ beamwidth can be (made) quite small at optical frequencies because of large electric dimension of the EM radiator

Unlike scattering theory, in geometric optics:

- A point in space receives power from a ray only if it lies along the propagation line of the ray
- Image theory significantly simplifies the analysis

Geometric Optics

Reflected electrical field:

$$E^{\text{lens}}(\mathbf{r}) = \sum_{\ell \mid \mathbf{r} \in \mathscr{A}_\ell} \sqrt{s^{\text{ray}}\left(E_\ell^{\text{irs}}\right)} \exp(jk|\mathbf{r} - \mathbf{p}_\ell|) \exp(j\phi_\ell),$$

- $E^{\text{lens}}(\mathbf{r})$: Electric field at the Rx lens at position $\mathbf{r}$
- E_ℓ^{irs}: Incident field on IRS for the ℓ-th ray
- $s^{\text{ray}}(\cdot)$: Power of the reflected ray
- $\mathbf{p}_\ell$: Position of the ℓ-th ray on the IRS
- ϕ_ℓ: Phase of the ℓ-th ray leaving the IRS
- $\mathscr{A}_\ell$: Points that lie along the propagation line of the ℓ-th ray

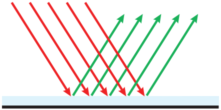

Specular reflection

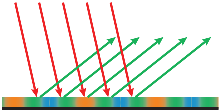

Anomalous reflection

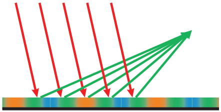

Focusing

Comparison of Analysis Methods

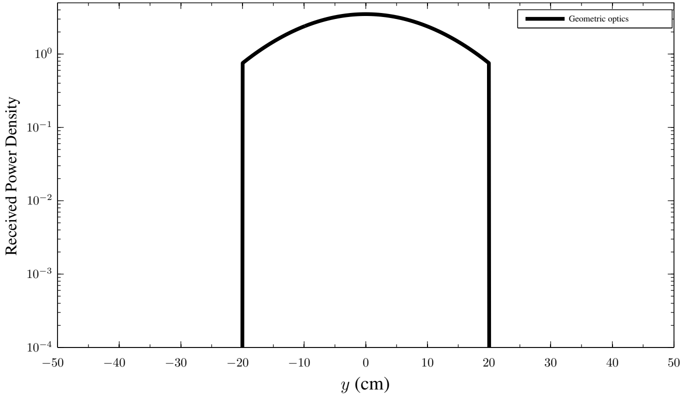

Received power density over the Rx lens line for the 2D setup. Setup: Reflecting a Gaussian beam from angle $\theta_i = \frac{\pi}{6}$ rad to angle $\theta_r = \theta_{rl} = 0$; $d_{sr} = d_{rl} = 200$ m; $w_0 = 1$ mm; $\lambda = 1550$ nm; $a_r = 10$ cm; $a_l = 2.5$ cm; $\varsigma = \sqrt{\cos(\theta_i)/\cos(\theta_r)}$, and the proposed phase-shift design in [R3].

Comparison of Analysis Methods

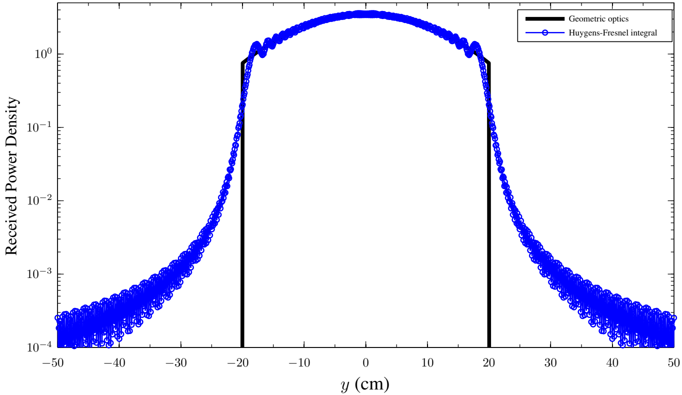

Received power density over the Rx lens line for the 2D setup. Setup: Reflecting a Gaussian beam from angle $\theta_i = \frac{\pi}{6}$ rad to angle $\theta_r = \theta_{rl} = 0$; $d_{sr} = d_{rl} = 200$ m; $w_0 = 1$ mm; $\lambda = 1550$ nm; $a_r = 10$ cm; $a_l = 2.5$ cm; $\varsigma = \sqrt{\cos(\theta_i)/\cos(\theta_r)}$, and the proposed phase-shift design in [R3].

Comparison of Analysis Methods

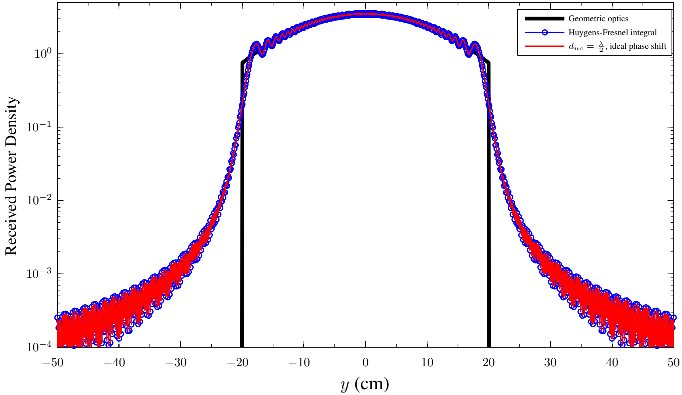

Received power density over the Rx lens line for the 2D setup. Setup: Reflecting a Gaussian beam from angle $\theta_i = \frac{\pi}{6}$ rad to angle $\theta_r = \theta_{rl} = 0$; $d_{sr} = d_{rl} = 200$ m; $w_0 = 1$ mm; $\lambda = 1550$ nm; $a_r = 10$ cm; $a_l = 2.5$ cm; $\varsigma = \sqrt{\cos(\theta_i)/\cos(\theta_r)}$, and the proposed phase-shift design in [R3].

Comparison of Analysis Methods

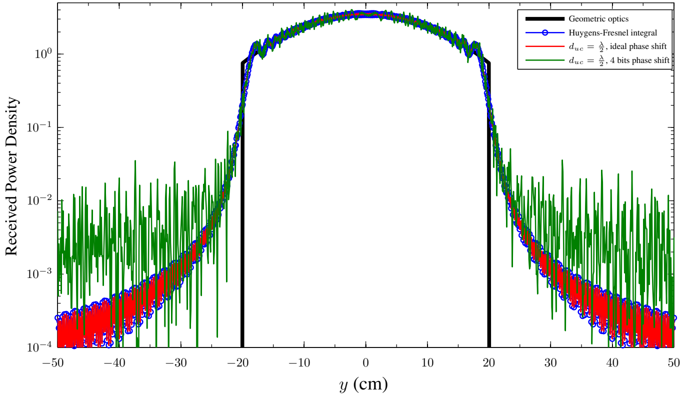

Received power density over the Rx lens line for the 2D setup. Setup: Reflecting a Gaussian beam from angle $\theta_i = \frac{\pi}{6}$ rad to angle $\theta_r = \theta_{rl} = 0$; $d_{sr} = d_{rl} = 200$ m; $w_0 = 1$ mm; $\lambda = 1550$ nm; $a_r = 10$ cm; $a_l = 2.5$ cm; $\varsigma = \sqrt{\cos(\theta_i)/\cos(\theta_r)}$, and the proposed phase-shift design in [R3].

Comparison of Analysis Methods

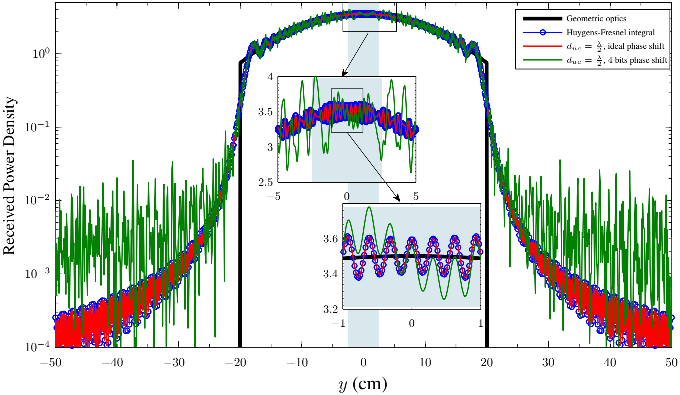

Received power density over the Rx lens line for the 2D setup. Setup: Reflecting a Gaussian beam from angle $\theta_i = \frac{\pi}{6}$ rad to angle $\theta_r = \theta_{rl} = 0$; $d_{sr} = d_{rl} = 200$ m; $w_0 = 1$ mm; $\lambda = 1550$ nm; $a_r = 10$ cm; $a_l = 2.5$ cm; $\varsigma = \sqrt{\cos(\theta_i)/\cos(\theta_r)}$, and the proposed phase-shift design in [R3].

IRS Area

Question: How much do we gain by increasing the IRS area considering

- A concentrated Gaussian beam
- An electrically-large receiving lens

Question: What is the impact of IRS design, e.g.:

- Specular reflection by a mirror
- Focusing by a meta-surface

Question: For what regime of IRS sizes does geometric-optic-based approximation become accurate?

Power Scaling Law

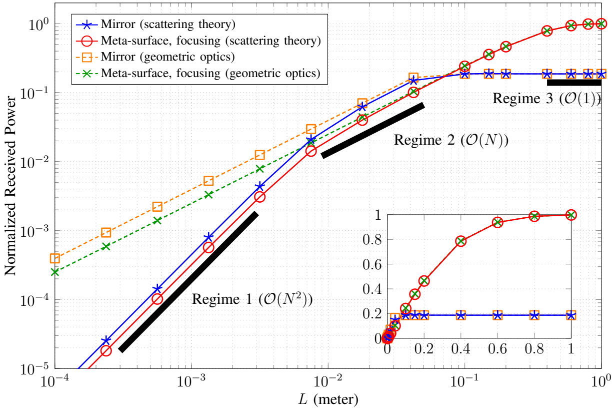

Fraction of transmit power received by an Rx lens vs. the IRS length L. Setup: 2D system; Tx at $(-200\text{ m}, 300\text{ m})$; IRS at $(0, 0)$, Rx at $(0, 500\text{ m})$; Gaussian beam; 1550 nm wavelength; waist radius $w_0 = 1$ mm; IRS length L; half-wavelength unit-cell spacing; Rx lens length 10 cm [R1].

4. Impact of Building Sway

Building Sway

- Building sway is caused by wind, thermal expansions, etc.
- Due to narrow laser beam, it causes beam misalignment or pointing error

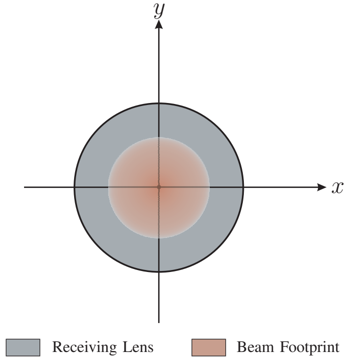

Building Sway

- Building sway is caused by wind, thermal expansions, etc.
- Due to narrow laser beam, it causes beam misalignment or pointing error

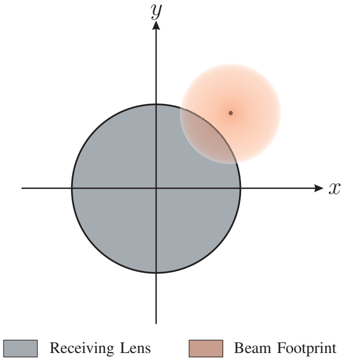

Building Sway

- Building sway is caused by wind, thermal expansions, etc.
- Due to narrow laser beam, it causes beam misalignment or pointing error

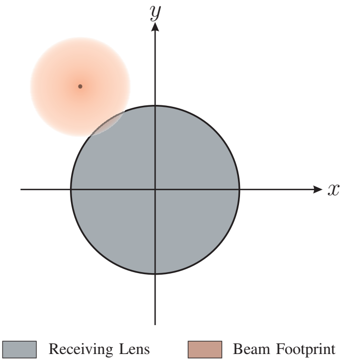

Statistical Model

The geometric loss h_g (i.e., the fraction of power reaching the receiving lens) is a random variable due to the random misalignment caused by building sway

Objective: Develop a statistical model of h_g that accounts for the sways of buildings where the transmitter, the IRS, and the receiver are placed on

Challenge: The models obtained based on scattering theory and Huygens-Fresnel principle are too complicated to serve as a basis for the derivation of a statistical model

Equivalent Mirror-assisted System

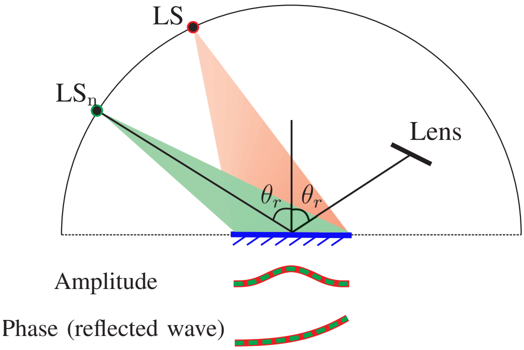

Helpful result [R3]: The IRS phase shift can be chosen such that the phase of the non-specular reflected wave from the IRS in the original system becomes identical to the phase of the (specular) reflected wave from a mirror in the equivalent system!

Equivalent Mirror-assisted System

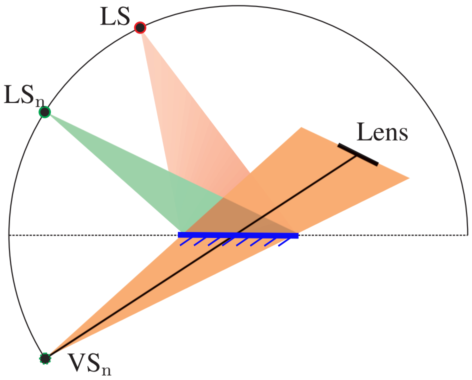

Analysis methods: This allows us to employ geometric optics and image theory to analyze the impact of building sway via the equivalent mirror-assisted system!

Deterministic Geometric Loss

For a given realization of misalignment vector **u**:

$$h_g = \iint_{(x,y)\in\mathscr{A}} I(x,y)\mathrm{d}x\mathrm{d}y$$

The solution to the above integral is not available in closed form!

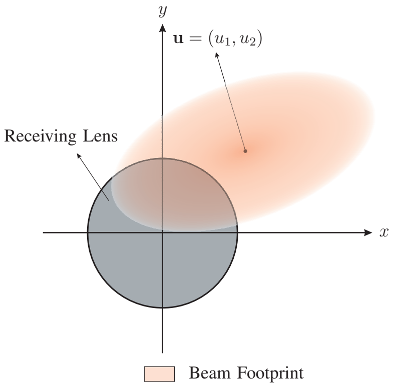

Deterministic Geometric Loss

Lower and upper bounds [R6]

$$h_g^{\text{low}} \approx A_0 \exp\left(-\frac{\|\mathbf{u}\|^2}{t_{\text{min}}}\right)$$

$$h_g^{\text{upp}} \approx A_0 \exp\left(-\frac{\|\mathbf{u}\|^2}{t_{\text{max}}}\right)$$

Proposed approximation:

$$h_g \approx A_0 \exp\left(-\frac{\|\mathbf{u}\|^2}{t}\right)$$

for some $t \in [t_{\text{min}}, t_{\text{max}}]$
Note: A_0, t_{min}, and t_{max} are derived in [R3] as functions of beam parameters!

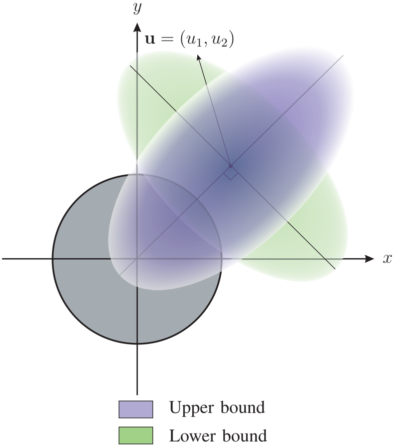

Statistical Misalignment Model

Assumption: 3D Gaussian building sway with independent components

- Tx: $\varepsilon_s^{x,y,z} \sim \mathcal{N}(\mathbf{0}, \sigma_s^2\mathbf{I})$
- IRS: $\varepsilon_r^{x,y,z} \sim \mathcal{N}(\mathbf{0}, \sigma_r^2\mathbf{I})$
- Rx: $\varepsilon_l^{x,y,z} \sim \mathcal{N}(\mathbf{0}, \sigma_l^2\mathbf{I})$

Statistical Misalignment Model

Assumption: 3D Gaussian building sway with independent components

- Tx: $\varepsilon_s^{x,y,z} \sim \mathcal{N}(\mathbf{0}, \sigma_s^2 \mathbf{I})$
- IRS: $\varepsilon_r^{x,y,z} \sim \mathcal{N}(\mathbf{0}, \sigma_r^2 \mathbf{I})$
- Rx: $\varepsilon_l^{x,y,z} \sim \mathcal{N}(\mathbf{0}, \sigma_l^2 \mathbf{I})$

Decoupling: For simplifications, we re-define $\varepsilon_s^{x,y,z}$, $\varepsilon_r^{x,y,z}$, and $\varepsilon_l^{x,y,z}$ in different coordinate systems

- Tx: $\varepsilon_s^{x,y,z}$ is decoupled into
  - ε_s^{xy}: components orthogonal to the direction of beam propagation
  - ε_s^{z}: component in the direction of beam propagation
- IRS: $\varepsilon_r^{x,y,z}$ is decoupled into
  - ε_r^{xy}: components in the IRS plane
  - ε_r^{z}: component orthogonal to the IRS plane
- Rx: $\varepsilon_r^{x,y,z}$ is decoupled into
  - ε_l^{xy}: components orthogonal to the direction of beam propagation
  - ε_l^{z}: component in the direction of beam propagation

For sufficiently large IRSs and large Rx-IRS and IRS-Rx distances, only ε_s^{xy}, ε_r^{z}, and ε_l^{xy} significantly contribute to the overall misalignment!

Statistical Geometric Loss Model

Assuming building sway variables ε_s^{xy}, ε_r^{z}, and ε_l^{xy} follow Gaussian distribution, $\|\mathbf{u}\|$ follows a Hoyt distribution and h_g follows the following distribution

$$f_{h_g}(h_g) = \frac{\varpi}{A_0}\left(\frac{h_g}{A_0}\right)^{\frac{(1+q^2)\varpi}{2q}-1} I_0\left(-\frac{(1-q^2)\varpi}{2q}\ln\left(\frac{h_g}{A_0}\right)\right), \quad 0 \leq h_g \leq A_0.$$

where $\varpi = \frac{(1+q^2)t}{4q\Omega}$ is a constant with

$$\Omega = \chi_1 + \chi_2 \quad \text{and} \quad q = \left[\frac{\min\{\chi_1, \chi_2\}}{\max\{\chi_1, \chi_2\}}\right]^{1/2},$$

where χ_1 and χ_2 are the eigenvalues of $\boldsymbol{\Sigma}$ [R3].

Simulation Results

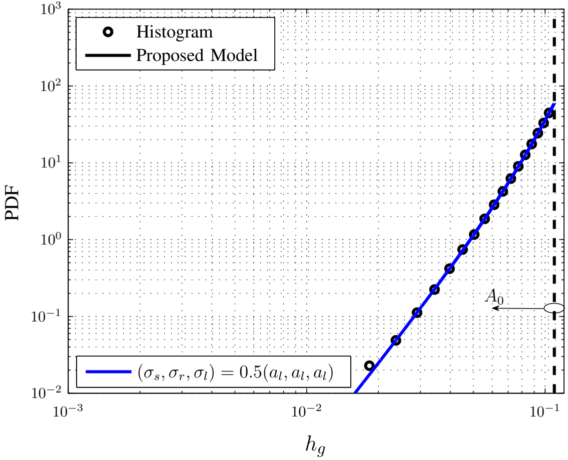

$(\sigma_s, \sigma_r, \sigma_l)$: building sway, $a_l = 2.5$ cm: lens radius [R3]

Simulation Results

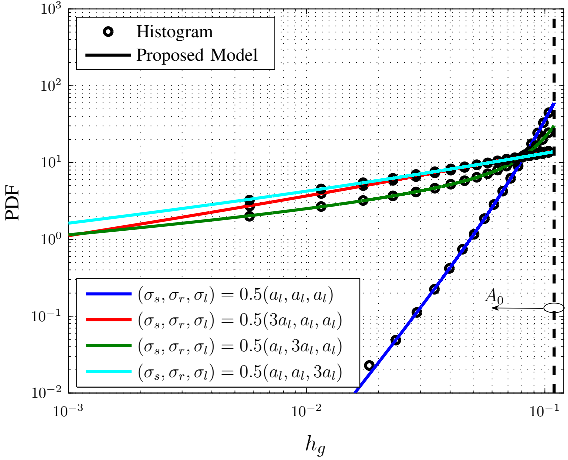

$(\sigma_s, \sigma_r, \sigma_l)$: building sway, $a_l = 2.5$ cm: lens radius [R3]

Simulation Results

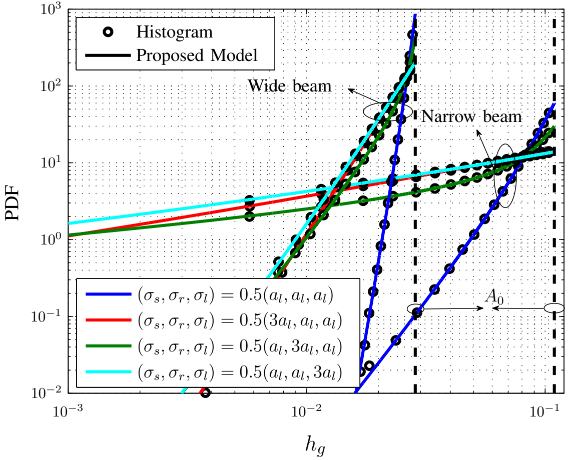

$(\sigma_s, \sigma_r, \sigma_l)$: building sway, $a_l = 2.5$ cm: lens radius [R3]

Simulation Results

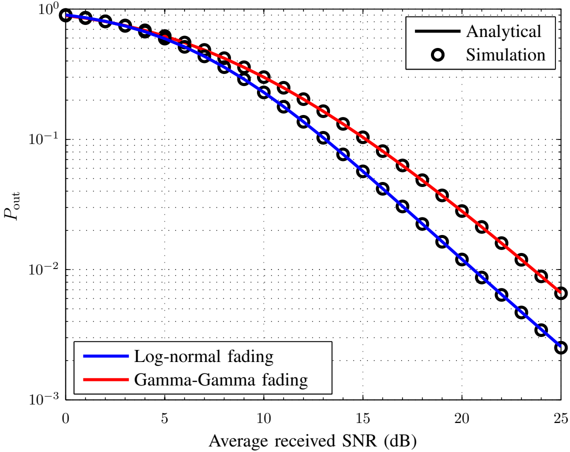

Simulation Results

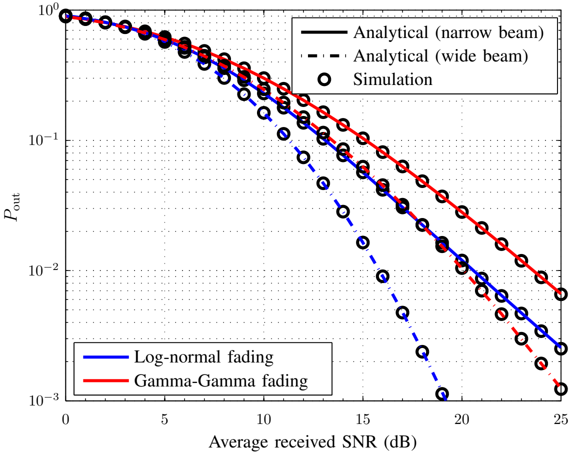

5. Multi-link FSO Systems

Multi-Link FSO Systems

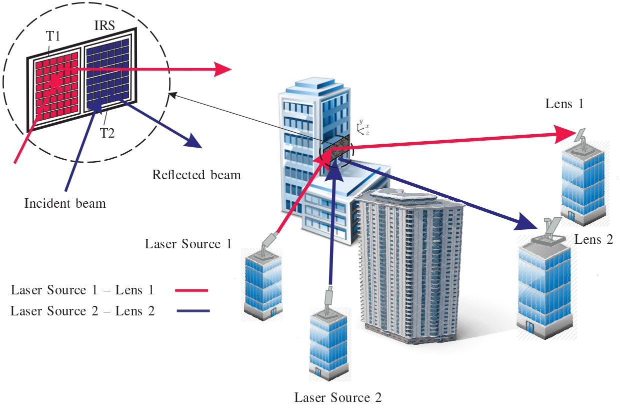

- Multiple LS-lens connections
- Single IRS for Gaussian FSO beams

Point-to-Point IRS-assisted FSO link

Repartition the IRS in to Q tiles which connects m-th LS to n-th lens

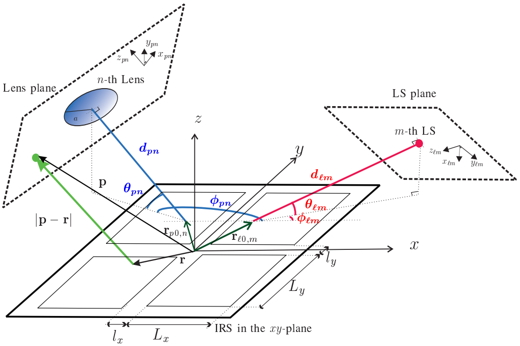

- Tile parameters: position (x_q, y_q), size (L_x, L_y), phase-shift profile $\Delta\phi_q(\mathbf{r})$
- LS and lens centers on the IRS: $\mathbf{r}_{\ell 0,m}$, $\mathbf{r}_{p0,n}$

Point-to-Point Geometric Loss

- **Point-to-point geometric loss** (*m*-th LS and *n*-th lens)

$$h_g^{m,n} = \iint\limits_{\mathscr{A}_{pn}} I^{m,n}(\mathbf{p}_n)\, \mathrm{d}\mathscr{A}_{pn}, \qquad I^{m,n}(\mathbf{p}_n) = \frac{\left|\sum_{q=1}^{Q} E_q^{m,n}(\mathbf{p}_n)\right|^2}{2\eta P_{\ell m}}$$

Point-to-Point Geometric Loss

- **Point-to-point geometric loss** (*m*-th LS and *n*-th lens)

$$h_g^{m,n} = \iint_{\mathscr{A}_{pn}} I^{m,n}(\mathbf{p}_n)\,\mathrm{d}\mathscr{A}_{pn}, \qquad I^{m,n}(\mathbf{p}_n) = \frac{\left|\sum_{q=1}^{Q} E_q^{m,n}(\mathbf{p}_n)\right|^2}{2\eta P_{\ell m}}$$

- **Huygens-Fresnel principle**

$$E_q^{\mathrm{m,n}}(\mathbf{p}_n) = \frac{\varsigma_q}{j\lambda}\int_{\mathbf{r}\in\mathscr{A}^{\mathrm{tile}}} E^{\mathrm{irs}}(\mathbf{r})\frac{\exp(jk|\mathbf{p}_n - \mathbf{r}|)}{|\mathbf{p}_n - \mathbf{r}|}\exp(j\Delta\phi_q(\mathbf{r}))\mathrm{d}\mathbf{r},$$

FRIEDRICH-ALEXANDER UNIVERSITÄT ERLANGEN-NÜRNBERG
FACULTY OF ENGINEERING

Point-to-Point Geometric Loss

- **Point-to-point geometric loss** (m-th LS and n-th lens)

$$h_g^{m,n} = \iint_{\mathscr{A}_{pn}} I^{m,n}(\mathbf{p}_n)\, \mathrm{d}\mathscr{A}_{pn}, \qquad I^{m,n}(\mathbf{p}_n) = \frac{\left|\sum_{q=1}^{Q} E_q^{m,n}(\mathbf{p}_n)\right|^2}{2\eta P_{\ell m}}$$

- **Huygens-Fresnel principle**

$$E_q^{\mathrm{m,n}}(\mathbf{p}_n) = \frac{\varsigma_q}{j\lambda} \int_{\mathbf{r}\in\mathscr{A}^{\mathrm{tile}}} E^{\mathrm{irs}}(\mathbf{r}) \frac{\exp(jk|\mathbf{p}_n - \mathbf{r}|)}{|\mathbf{p}_n - \mathbf{r}|} \exp(j\Delta\phi_q(\mathbf{r}))\mathrm{d}\mathbf{r},$$

- To find closed form solution, approximate $|\mathbf{p}_n - \mathbf{r}|$ as

$$|\mathbf{p}_n - \mathbf{r}| \approx \underbrace{|\mathbf{p}_n| - \frac{xp_x + yp_y}{|\mathbf{p}_n|}}_{=\mathrm{t}_1} + \underbrace{\frac{x^2 + y^2}{2|\mathbf{p}_n|} - \frac{x^2p_x^2 + y^2p_y^2}{2|\mathbf{p}_n|^3}}_{=\mathrm{t}_2}$$

Far-Field vs. Intermediate-Field

- **Far-field regime** (term t_1) [R4]

$$k\frac{x^2+y^2}{2|\mathbf{p}_n|} \ll 2\pi \rightarrow d_f = \frac{x_e^2+y_e^2}{2\lambda}$$

where $x_e = \min\left(\frac{L_x}{2}, w_x\right)$ and $y_e = \min\left(\frac{L_y}{2}, w_y\right)$.

Far-Field vs. Intermediate-Field

- **Far-field regime** (term t_1) [R4]

$$k\frac{x^2+y^2}{2|\mathbf{p}_n|} \ll 2\pi \rightarrow d_f = \frac{x_e^2+y_e^2}{2\lambda}$$

where $x_e = \min\left(\frac{L_x}{2}, w_x\right)$ and $y_e = \min\left(\frac{L_y}{2}, w_y\right)$.

- **Intermediate-field regime** (terms t_1 and t_2) [R4]

$$k\frac{(x^2+y^2)(xp_x+yp_y)}{2|\mathbf{p}_n|^3} \ll 2\pi \rightarrow d_n = \left[\frac{(x_e^2+y_e^2)(x_e+y_e)}{4\lambda}\right]^{1/2}$$

Far-Field vs. Intermediate-Field

- **Far-field regime** (term t_1) [R4]

$$k\frac{x^2+y^2}{2|\mathbf{p}_n|} \ll 2\pi \rightarrow d_f = \frac{x_e^2+y_e^2}{2\lambda}$$

where $x_e = \min\left(\frac{L_x}{2}, w_x\right)$ and $y_e = \min\left(\frac{L_y}{2}, w_y\right)$.

- **Intermediate-field regime** (terms t_1 and t_2) [R4]

$$k\frac{(x^2+y^2)(xp_x+yp_y)}{2|\mathbf{p}_n|^3} \ll 2\pi \rightarrow d_n = \left[\frac{(x_e^2+y_e^2)(x_e+y_e)}{4\lambda}\right]^{1/2}$$

- **Example:** IRS with $L_x = L_y = 50$ cm and LS at $(d_\ell, \theta_\ell, \phi_\ell) = \left(1000\,\mathrm{m}, \frac{\pi}{8}, 0\right)$ with $\lambda = 1550$ nm and $w_0 = 2.5$ mm

$$\boxed{d_f = 32.7 \times 10^3\,\mathrm{m} \quad \text{and} \quad d_n = 85.6\,\mathrm{m}}$$

Far-Field vs. Intermediate-Field

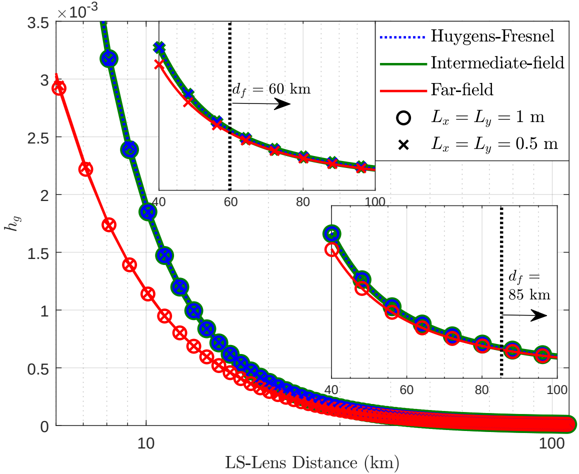

$L_x \times L_y$: IRS size [R5]

Multi-Link IRS-Assisted FSO Systems

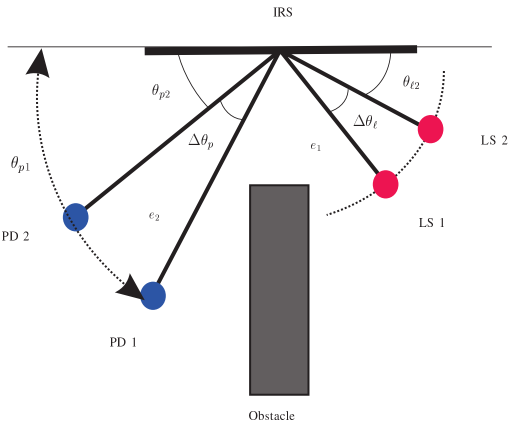

Share an IRS among multiple FSO links $\Leftrightarrow$ Impact of misalignment errors, delay, received power, and inter-link interference

IRS Sharing Protocols

- **Protocols [R5]**

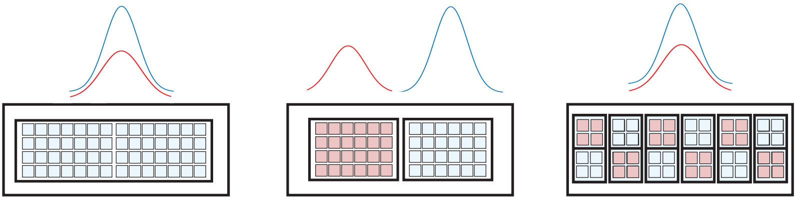

a) Time Division (TD) b) IRS Division (IRSD) c) IRS Homogenization (IRSH)

- **Parameters**
  - Number of tiles (Q)
  - Tile phase shift profile ($\mathbf{r}_q^t$)
  - LS footprint center ($\mathbf{r}_{\ell 0}$)
  - Lens center on the IRS ($\mathbf{r}_{p0}$)

Table: IRS sharing protocols parameters.

Sharing Protocols	Q	$\mathbf{r}_q^t$	$\mathbf{r}_{\ell 0}$,$\mathbf{r}_{p0}$
TD protocol	1	$(0,0)$	$(0,0)$
IRSD protocol	N	$\mathbf{r}_q$	$\mathbf{r}_q$
IRSH protocol	$\gg N$	$(0,0)$	$(0,0)$

Simulation Results

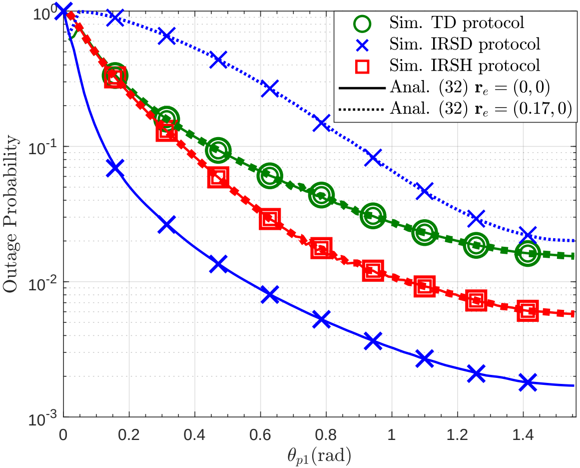

Target rate: $R = 1.7$ Gbit/s [R5]

Simulation Results

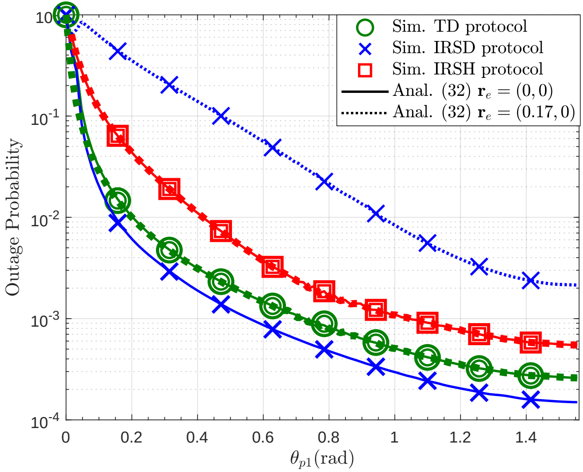

Target rate: $R = 0.5$ Gbit/s [R5]

6. Conclusions and Future Work

Summary and Conclusions

- **Optical IRSs**
  - Review and comparison of different optical IRS technologies
  - Comparison of IRS-assisted RF and FSO systems
- **Deterministic channel model**
  - Geometric loss
  - Comparison of different analysis methods
- **Statistical channel model**
  - Building sway
  - Equivalent mirror-assisted analysis
- **Multi-link FSO systems**

Summary and Conclusions

- **Optical IRSs**
  - Review and comparison of different optical IRS technologies
  - Comparison of IRS-assisted RF and FSO systems
- **Deterministic channel model**
  - Geometric loss
  - Comparison of different analysis methods
- **Statistical channel model**
  - Building sway
  - Equivalent mirror-assisted analysis
- **Multi-link FSO systems**

Take-away messages:

- Optical IRSs can be used to relax the LoS requirement, which is a persisting limitation of FSO systems
- Optical IRS-assisted systems have unique features different from RF IRS-assisted systems; hence new design and analysis methods are needed
- Compared to RF IRSs, optical IRSs are relatively less studied from a communication-theoretical perspective; many open problems exist

Future Work

- **Channel modeling**
  - Geometric loss for general phase-shift models
  - Pointing error for a given IRS design (e.g., focusing, collimation, etc.)
  - Channel delay dispersion
  - Wavefront distortion
- **System design and performance analysis**
  - Initial link establishment
  - Channel estimation
  - Modulation schemes
  - IRS optimization
- **Implementation**
  - Relevant hardware constraints/impairments
  - Verification of the theory via experiments

References

References for Further Reading I

Overview paper on IRS-assisted FSO systems:

[R1] V. Jamali, H. Ajam, M. Najafi, B. Schmauss, R. Schober, and H. V. Poor, "Intelligent Reflecting Surface-assisted Free-space Optical Communications," *Accepted for Publication in IEEE Communications Magazine*, 2021.

Mirror-assisted FSO systems (deterministic and statistical models):

[R2] M. Najafi and R. Schober, "Intelligent Reflecting Surfaces for Free Space Optical Communications," *IEEE Global Communications Conference*, pp. 1-7, Dec. 2019.

Meta-surface-assisted FSO systems (deterministic and statistical models using geometric optic-based analysis):

[R3] M. Najafi, B. Schmauss, and R. Schober, "Intelligent Reconfigurable Reflecting Surfaces for Free Space Optical Communications," *IEEE Transactions on Communications*, vol. 69, no. 9, pp. 6134-6151, Sept. 2021.

References for Further Reading II

Meta-surface-assisted FSO systems (deterministic model using Huygens-Fresnel principle-based analysis):

[R4] H. Ajam, M. Najafi, V. Jamali, and R. Schober, "Channel Modeling for IRS-assisted FSO Systems," *IEEE Wireless Communications and Networking Conference*, pp. 1-7, March 2021.

Meta-surface-assisted multi-link FSO systems (deterministic model using Huygens-Fresnel principle-based analysis):

[R5] H. Ajam, M. Najafi, V. Jamali, and R. Schober, "Modeling and Design of IRS-Assisted Multi-Link FSO Systems," *Submitted to IEEE Transactions on Communications*.

Derivation of the lower and upper bounds on the geometric loss for a beam footprint on the receiving lens plane with a rotated elliptical power contours:

[R6] M. Najafi, H. Ajam, V. Jamali, P. D. Diamantoulakis, G. K. Karagiannidis, and R. Schober. "Statistical Modeling of the FSO Fronthaul Channel for UAV-based Communications," *IEEE Transactions on Communications*, vol. 68, no. 6, pp. 3720-3736, Jun. 2020.

Thank you for your attention!
Questions?

Optical IRSs vs. Optical Relays

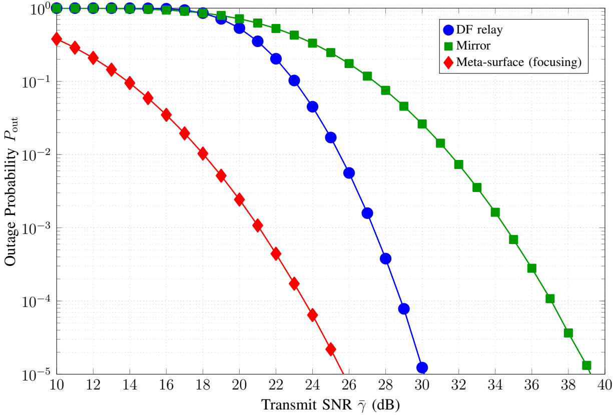

Optical IRSs vs. Optical Relays